



## RESEARCH LETTER

10.1002/2017GL076253

## Key Points:

- A portion of the  $\delta^{18}\text{O}$  signal in land-based paleoclimate proxies can be attributed to the direct meltwater effect instead of climatic changes
- The direct meltwater effect can make up 15–35% of the  $\delta^{18}\text{O}$  signals in precipitation in Greenland and eastern Brazil for large meltwater events
- The direct meltwater effect increases with the magnitude and duration of the freshwater forcing and is sensitive to location and shape dependent

## Supporting Information:

- Supporting Information S1

## Correspondence to:

J. Zhu,  
jzhu47@wisc.edu

## Citation:

Zhu, J., Liu, Z., Brady, E. C., Otto-Bliesner, B. L., Marcott, S. A., Zhang, J., ... Noone, D. (2017). Investigating the direct meltwater effect in terrestrial oxygen-isotope paleoclimate records using an isotope-enabled Earth system model. *Geophysical Research Letters*, *44*, 12,501–12,510. <https://doi.org/10.1002/2017GL076253>

Received 7 NOV 2017

Accepted 10 DEC 2017

Accepted article online 14 DEC 2017

Published online 28 DEC 2017

## Investigating the Direct Meltwater Effect in Terrestrial Oxygen-Isotope Paleoclimate Records Using an Isotope-Enabled Earth System Model

Jiang Zhu<sup>1,2</sup> , Zhengyu Liu<sup>3</sup> , Esther C. Brady<sup>4</sup> , Bette L. Otto-Bliesner<sup>4</sup> , Shaun A. Marcott<sup>5</sup> , Jiaxu Zhang<sup>6</sup> , Xianfeng Wang<sup>7</sup> , Jesse Nusbaumer<sup>8</sup> , Tony E. Wong<sup>9</sup> , Alexandra Jahn<sup>10</sup> , and David Noone<sup>11</sup>

<sup>1</sup>Department of Atmospheric and Oceanic Sciences and Center for Climatic Research, University of Wisconsin-Madison, Madison, WI, USA, <sup>2</sup>Now at Department of Earth and Environmental Sciences, University of Michigan, Ann Arbor, MI, USA, <sup>3</sup>Atmospheric Science Program, Department of Geography, Ohio State University, Columbus, OH, USA, <sup>4</sup>Climate and Global Dynamics Laboratory, National Center for Atmospheric Research, Boulder, CO, USA, <sup>5</sup>Department of Geoscience, University of Wisconsin-Madison, Madison, WI, USA, <sup>6</sup>CCS-2 and CNLS, Los Alamos National Laboratory, Los Alamos, NM, USA, <sup>7</sup>Earth Observatory of Singapore and Asian School of the Environment, Nanyang Technological University, Singapore, <sup>8</sup>NASA Goddard Institute for Space Studies, New York, NY, USA, <sup>9</sup>Department of Computer Science, University of Colorado Boulder, Boulder, CO, USA, <sup>10</sup>Department of Atmospheric and Oceanic Sciences and Institute of Arctic and Alpine Research, University of Colorado Boulder, Boulder, CO, USA, <sup>11</sup>College of Earth, Ocean, and Atmospheric Sciences, Oregon State University, Corvallis, OR, USA

**Abstract** Variations in terrestrial oxygen-isotope reconstructions from ice cores and speleothems have been primarily attributed to climatic changes of surface air temperature, precipitation amount, or atmospheric circulation. Here we demonstrate with the fully coupled isotope-enabled Community Earth System Model an additional process contributing to the oxygen-isotope variations during glacial meltwater events. This process, termed “the direct meltwater effect,” involves propagating large amounts of isotopically depleted meltwater throughout the hydrological cycle and is independent of climatic changes. We find that the direct meltwater effect can make up 15–35% of the  $\delta^{18}\text{O}$  signals in precipitation over Greenland and eastern Brazil for large freshwater forcings (0.25–0.50 sverdrup ( $10^6 \text{ m}^3/\text{s}$ )). Model simulations further demonstrate that the direct meltwater effect increases with the magnitude and duration of the freshwater forcing and is sensitive to both the location and shape of the meltwater. These new modeling results have important implications for past climate interpretations of  $\delta^{18}\text{O}$ .

### 1. Introduction

Oxygen isotope ratios (typically reported as  $\delta^{18}\text{O}$ ) in terrestrial paleoclimate archives have long been used to study the climate evolution of the late Quaternary (e.g., Jouzel et al., 1997; Y. Wang et al., 2001). The  $\delta^{18}\text{O}$  signals in ice cores and terrestrial speleothems have primarily been interpreted as changes in surface air temperature and regional precipitation amount, respectively, based on the high-latitude “temperature effect” and the tropical “amount effect” (Dansgaard, 1964; Rozanski et al., 1993). Later studies, however, point to more complex and nuanced interpretations in which the  $\delta^{18}\text{O}$  signal from ice cores reflects changes in moisture sources (Charles et al., 1994; Liu et al., 2012), atmospheric circulation and weather processes (Hendricks et al., 2000; Lee et al., 2007; Noone, 2008), sea ice margin positions (Sime et al., 2013), and postdepositional processes (Steen-Larsen et al., 2014; Town et al., 2008). Likewise,  $\delta^{18}\text{O}$  variations in speleothem records have also been related to changes in initial vapor source composition and transport trajectory (Lewis et al., 2010; Liu et al., 2014; Rozanski et al., 1993; Yuan et al., 2004), changes in seasonality (Cheng et al., 2009), the proportion of convective and stratiform precipitation (Aggarwal et al., 2016), and numerous cloud-scale processes (Moore et al., 2014; Risi et al., 2008).

Of all these influences on the  $\delta^{18}\text{O}$  signals, the dominant effects are largely explained by changes in climate. However, large glacial meltwater events also serve as a nonclimatic driver of terrestrial  $\delta^{18}\text{O}$  variability. The glacial meltwater discharged into the northern North Atlantic Ocean by icebergs or surface runoff is considerably depleted in  $\delta^{18}\text{O}$  ( $\delta^{18}\text{O} \sim -30$  to  $-50\text{‰}$ ) compared to the surface ocean (Hillaire-Marcel & Causse, 1989; Sima et al., 2006). This isotopically depleted meltwater can significantly decrease the isotope composition of the seawater into which it deposits (e.g., Bagniewski et al., 2015; Bagniewski, Meissner, & Menviel,

2017; LeGrande & Schmidt, 2008; Roche et al., 2014) and can further propagate throughout the hydrological cycle to directly influence the  $\delta^{18}\text{O}$  values in adjacent terrestrial paleoclimate archives. We term this process “the direct meltwater effect,” as it directly influences the  $\delta^{18}\text{O}$  signals through changes in water mixing alone. By contrast, “indirect climate effects” involve changes in climate state that then influence the  $\delta^{18}\text{O}$  signals. As a result, part of the variations in some terrestrial oxygen-isotope records during meltwater events, such as Heinrich events, likely reflect both of these direct and indirect meltwater signals. Werner, Mikolajewicz, Hoffmann, and Heimann (2000) and LeGrande and Schmidt (2008) noticed this direct meltwater effect in precipitation-derived  $\delta^{18}\text{O}$  in their isotope-enabled models, but its impact on the terrestrial  $\delta^{18}\text{O}$  records has not been quantified. Importantly, it still remains unclear how large the direct meltwater effect is relative to the climatic effect and how this effect depends on the characteristics of the freshwater forcing, for example, the magnitude, location, and duration. The dependence on the characteristics of the freshwater forcing is of particular interest to improve interpretations of terrestrial  $\delta^{18}\text{O}$  records, especially considering the large uncertainties in past meltwater events (Clark et al., 2001).

In this study, we make the first attempt to quantify the importance of the direct meltwater effect in terrestrial  $\delta^{18}\text{O}$  records and investigate its dependence on the amount, location, and duration of the freshwater forcing using a suite of water hosing experiments with a fully coupled water isotope-enabled Earth system model. We focus our study on Greenland and eastern Brazil where multiple ice core and terrestrial speleothem  $\delta^{18}\text{O}$  records have been collected and used to reconstruct late Quaternary climate (e.g., Cruz et al., 2006, 2009; Johnsen et al., 2001; Stríkis et al., 2015; X. Wang et al., 2007).

## 2. Model and Experiments

We employ the recently developed fully coupled water isotope-enabled Community Earth System Model version 1.3 (iCESM). The model has a similar physical climate as the CESM1 (Hurrell et al., 2013) but with the capability to explicitly simulate the water isotopes in each component—the atmosphere, land, ocean, sea ice, and river runoff (Nusbaumer et al., 2017; Wong et al., 2017; Zhang et al., 2017; Zhu et al., 2017). All our simulations were conducted using the iCESM with a horizontal resolution of  $1.9 \times 2.5^\circ$  (latitude  $\times$  longitude) for the atmosphere and land and a nominal  $1^\circ$  for the ocean and sea ice. A preindustrial control simulation was run for 500 years, with forcing fixed at the values from 1850 A.D. and water isotopes in the ocean initialized from the Goddard Institute for Space Studies observationally interpolated seawater  $\delta^{18}\text{O}$  data set (LeGrande & Schmidt, 2006).

A suite of idealized water hosing experiments with different freshwater forcing (Table 1) was carried out following previous studies (e.g., Brady & Otto-Bliesner, 2011; Otto-Bliesner & Brady, 2010; Stouffer et al., 2006) applying the input of isotopically depleted freshwater at the surface ocean (LeGrande et al., 2006). For example, 0.25 sverdrup (Sv) ( $10^6 \text{ m}^3/\text{s}^1$ ) meltwater with a  $\delta^{18}\text{O}$  value of  $-30\text{‰}$  (Hillaire-Marcel & Causse, 1989; Sima et al., 2006) was applied evenly in the northern North Atlantic Ocean ( $50\text{--}70^\circ\text{N}$ ) for 300 years in experiment WH025a. The value of 0.25 Sv is chosen to represent a typical large meltwater event, for example, during Heinrich events (Hemming, 2004; Roche et al., 2014). Importantly, to separate the direct meltwater effect from the indirect climatic  $\delta^{18}\text{O}$  changes, a parallel water hosing experiment (WH025aC) was carried out with a meltwater  $\delta^{18}\text{O}$  of zero. Any difference in  $\delta^{18}\text{O}$  between WH025a and WH025aC isolates the contribution of the direct meltwater effect, which is generated by the propagation of isotopically depleted meltwater directly through the hydrological cycle without involving changes in the physical climate. To study the sensitivity of the direct meltwater effect to the magnitude of freshwater forcing, additional 100 yearlong experiments with 0.10, 0.50, and 1.00 Sv of meltwater were performed (Table 1). To explore the sensitivity of the direct meltwater effect to the location of freshwater forcing, another set of experiments were performed with 0.50 Sv of meltwater being discharged for 100 years into the Gulf of Mexico and the Weddell Sea, instead of the northern North Atlantic.

We investigate the direct meltwater effect in terrestrial oxygen-isotope records (e.g., ice cores and speleothems) using modeled annual mean  $\delta^{18}\text{O}$  in precipitation ( $\delta^{18}\text{O}_p$ ), weighted by the monthly precipitation amounts. For illustrative purpose, the direct meltwater effect in Greenland ice core and eastern Brazil speleothem records is discussed in detail, but results can be generalized to other regions and other kinds of oxygen-isotope paleoclimate records.

**Table 1**  
List of Experiments in This Study

Experiment	MWF	$\delta^{18}\text{O}$ of meltwater	Location	Length	AMOC	Greenland $T$ and $\Delta T$
PI	---	---	---	500	24.2	-26.0
WH010a	0.10	-30	N. Atlantic	100	17.5	-4.3
WH010aC	0.10	0	N. Atlantic	100	17.5	-4.3
WH025a	0.25	-30	N. Atlantic	300	5.7	-9.4
WH025aC	0.25	0	N. Atlantic	300	5.7	-9.4
WH050a	0.50	-30	N. Atlantic	100	2.8	-9.2
WH050aC	0.50	0	N. Atlantic	100	2.8	-9.2
WH100a	1.00	-30	N. Atlantic	100	2.6	-9.5
WH100aC	1.00	0	N. Atlantic	100	2.6	-9.5
WH050b	0.50	-30	Gulf of Mexico	100	8.5	-7.6
WH050bC	0.50	0	Gulf of Mexico	100	8.5	-7.6
WH050c	0.50	-30	Weddell Sea	100	22.3	-0.6
WH050cC	0.50	0	Weddell Sea	100	22.3	-0.6

Note. Details include the experiment name, magnitude of freshwater forcing (Sv),  $\delta^{18}\text{O}$  value of the meltwater (‰ with respect to Vienna Standard Mean Ocean Water, VSMOW), location of the freshwater forcing, length of the simulation (year), the AMOC strength (Sv), and Greenland temperature changes (°C) at year 100 in the simulations. We applied the forcing in the following regions: the N. Atlantic, 50–70°N; the Gulf of Mexico, 15–33°N, 255–279°E; and the Weddell Sea, 60–80°S, 290°E–30°E.

### 3. Climate and $\delta^{18}\text{O}$ Response to Freshwater Forcing

In WH025a, the maximum strength of the Atlantic Meridional Overturning Circulation (AMOC) decreases by 76% from 24.2 to 5.7 Sv in the first 100 years (Table 1 and Figure S1 in the supporting information). As a result of the reduced northward oceanic heat transport, the surface air temperature exhibits the expected bipolar seesaw response (Figure S2 in the supporting information) (Broecker, 1992). Along with the bipolar seesaw in surface temperature, there is a clear southward shift of the Intertropical Convergence Zone (ITCZ) in WH025a, especially over the Atlantic sector (Figure S2). In general, the AMOC intensity and the climate characters (e.g., Greenland surface temperature and precipitation amount over eastern Brazil) respond more strongly and rapidly to a larger magnitude of freshwater forcing in the northern North Atlantic, but the climate response seems to saturate beyond 0.25 Sv (Figure S1). Furthermore, meltwater discharged into the Gulf of Mexico also weakens the AMOC significantly but with a slower response (e.g., WH050a versus WH050b; Figure S1). The AMOC intensity and Greenland temperature only decrease slightly in the first 100 years if the freshwater forcing is applied to the Weddell Sea (Figure S1). These climate responses and their sensitivity to the characteristics of freshwater forcing are similar to previous idealized water hosing experiments (Brady & Otto-Bliesner, 2011; He, 2011; Otto-Bliesner & Brady, 2010; Stouffer et al., 2006).

In response to the isotopically depleted freshwater forcing in WH025a,  $\delta^{18}\text{O}$  in seawater ( $\delta^{18}\text{O}_{\text{sw}}$ ) decreases significantly in the surface ocean, especially locally in the northern North Atlantic where the maximum decrease exceeds 4‰ in 100 years (Figure S2). The depleted seawater is carried northward into the Arctic Ocean and southward into the subtropical and equatorial Atlantic by the gyre circulations. The evaporation over ocean further disperses the  $^{18}\text{O}$ -depleted meltwater signal into the atmosphere and then the nearby continents through precipitation. Our experiments (WH025a and WH050a) capture the major pattern of abrupt changes in terrestrial  $\delta^{18}\text{O}$  records reasonably well (Figure 1), including the marked decrease of  $\delta^{18}\text{O}$  in Greenland ice cores (Figure 1a) (Johnsen et al., 2001), a decrease of  $\delta^{18}\text{O}$  in eastern Brazil stalagmite records (Figure 1d) (Cruz et al., 2006, 2009; Strikis et al., 2015; X. Wang et al., 2007), an enrichment in southern China stalagmite records (Y. Wang et al., 2008; Y. J. Wang et al., 2001; Zhou et al., 2008), and speleothem records in the western Pacific Warm Pool and lake sediment data in tropical Southeast Africa (Figure S4 in the supporting information) (Carolin et al., 2013; Partin et al., 2007; Tierney et al., 2008). A detailed comparison between the model-simulated responses in  $\delta^{18}\text{O}$  (with temperature-induced fractionation corrected using Kim & O’Neil, 1997) and the compilation of speleothem records during Heinrich events (Lewis et al., 2010) can be found in the supporting information (Text S3 and Figure S3). Overall, the model can reproduce the  $\delta^{18}\text{O}$  changes during Heinrich events in speleothem records over East Asia and eastern Brazil remarkably well, with a correlation coefficient close to 0.9.

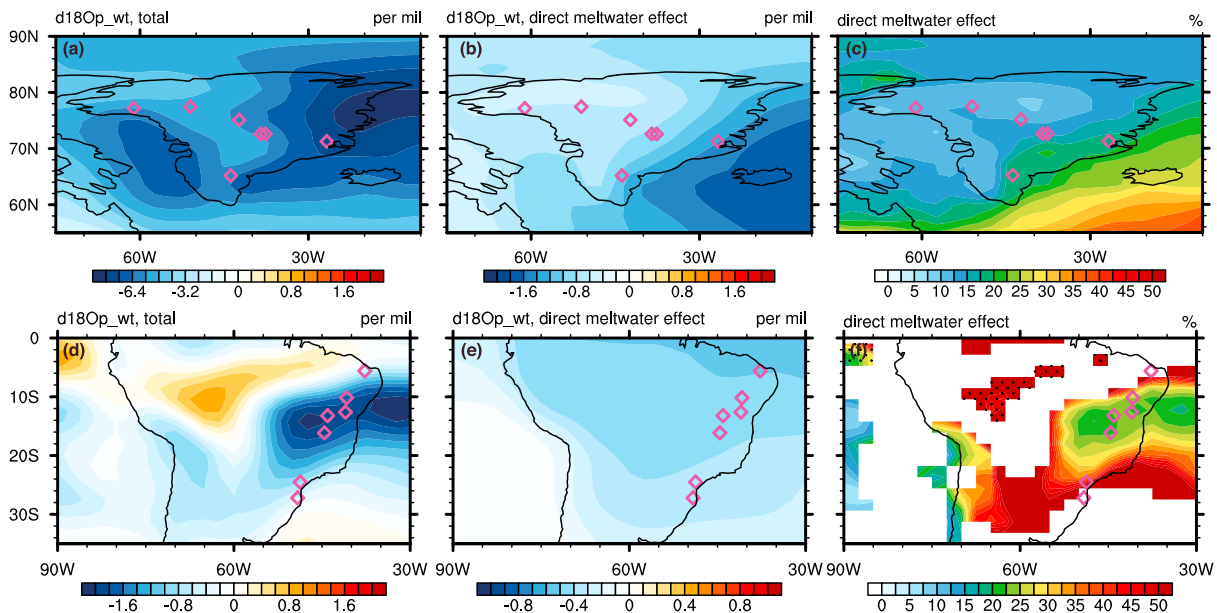


**Figure 1.** (a) Total changes of the simulated annual mean  $\delta^{18}\text{O}$  in precipitation in WH025a, (b) contribution by the direct meltwater effect, and (c) the direct meltwater effect in percentage over Greenland. (d, e, f) The same as Figures 1a–1c but for eastern Brazil. Markers in the map denote locations of related oxygen-isotope records in the literature. For Figures 1c and 1f, only regions with total changes in Figures 1a and 1d larger than the internal variability (one standard deviation) are filled. Regions with the direct meltwater effect opposite to the total changes are dotted. Note that color bar for Figure 1a is not equally spaced. Calculations are based on model output averaged between model years 271 and 300 in WH025a.

#### 4. The Direct Meltwater Effect

Our experimental setup (e.g., WH025a versus WH025aC) enables us to separate the direct meltwater effect from the indirect climate effects during meltwater events. We find that the direct meltwater effect contributes a substantial portion, as large as 20%, to the total depletion of  $\delta^{18}\text{O}_p$  in Greenland ice cores in response to the 0.25 Sv freshwater forcing in 300 years (Figures 1a–1c). Over the Greenland Summit, the total decrease of  $\delta^{18}\text{O}$  reaches  $-6\text{‰}$ . Out of this decrease, about  $-0.8$  to  $-1.0\text{‰}$  can be explained by the transport of  $^{18}\text{O}$ -depleted meltwater from the northern North Atlantic by the atmospheric circulations, without involving any variations in local temperature. The direct meltwater effect reaches a maximum in southeastern Greenland (e.g., about 20% at the Renland and Dye 3 sites) and decreases toward the northwest (e.g., 10% at the Camp Century site). These results suggest that attributing the  $\delta^{18}\text{O}$  signal in Greenland (e.g., Andersen et al., 2004; Grootes et al., 1993; NEEM community members, 2013) as a simple climate response (i.e., decrease in surface air temperature) during large meltwater events (Clark et al., 2004; Heinrich, 1988) could overestimate the  $\delta^{18}\text{O}$  signal and surface air temperature cooling, especially for cores in southeast Greenland.

The direct meltwater effect is not restricted to Greenland alone and is also significant in eastern Brazil (Figures 1d–1f;  $5\text{--}30^\circ\text{S}$ ,  $35\text{--}55^\circ\text{W}$ ), where speleothem-based oxygen-isotope records have been used to study the past evolution of the South American Monsoon (Cruz et al., 2006, 2009; Strikis et al., 2015; X. Wang et al., 2007). Specifically, a  $\delta^{18}\text{O}$  depletion of  $1.0\text{--}1.6\text{‰}$  during Heinrich events has been reported in eastern Brazil speleothem records and has been interpreted as an increase of regional rainfall amount associated with a southward shift of the ITCZ (Cruz et al., 2006, 2009; Strikis et al., 2015; X. Wang et al., 2007). In WH025a, the average  $\delta^{18}\text{O}_p$  depletion in 300 years is about  $1.5\text{‰}$  in eastern Brazil, agreeing quantitatively with these speleothem records (see also detailed model-data comparison in Figure S3 and Text S3). However, the additional water hosing experiment (WH025aC) suggests that 20–35% ( $\sim 0.4\text{‰}$ ) of the  $\delta^{18}\text{O}_p$  depletion after 300 years is from the direct meltwater effect, indicating that changes in the  $\delta^{18}\text{O}$  climate response during meltwater events may not be as large as previously assumed.

The significance of the direct meltwater effect extends beyond Greenland and eastern Brazil to other regions, such as North America, Europe, and Asia. In WH025a, the direct meltwater effect over North America and

Europe is larger than 50%, with the total  $\delta^{18}\text{O}_p$  depletion in these regions around 1.0‰ (Figure S4). It is also important to note that the direct meltwater effect can be opposite in sign to the indirect climate effects. For example, over the Caribbean region, the enrichment of  $\delta^{18}\text{O}_p$  caused by the indirect climate effects (shift of the ITCZ) is 0.8–1.6‰, and the depletion caused by the direct meltwater effect is –0.6 to –0.8‰ (Figure S4). As a result, the total  $\delta^{18}\text{O}_p$  changes is only ~0.5‰, revealing that the climate signal has been damped by the direct meltwater effect by more than 50%. Similarly, in the East and South Asian Monsoon region, total  $\delta^{18}\text{O}_p$  enrichment in response to the freshwater forcing in the North Atlantic can also be offset by the direct meltwater effect, albeit only by a small amount (5–10%).

## 5. Dependence of the Direct Meltwater Effect on Characteristics of Freshwater Forcing

How does the magnitude of the direct meltwater effect vary with the amount, location, and duration of the meltwater discharged into the ocean? Figure 2 summarizes the importance of the direct meltwater effect in  $\delta^{18}\text{O}_p$  in Greenland and eastern Brazil at year 100 of water hosing experiments (Table 1). The total depletion of  $\delta^{18}\text{O}_p$  in both Greenland and eastern Brazil increases with the amount of meltwater discharged into the northern North Atlantic (Figures 2a and 2d). However, the contribution by the direct meltwater effect increases almost linearly with the meltwater amount, so that its percentage increasing is proportional to the magnitude of the freshwater forcing (Figures 2b and 2e). Over Greenland the direct meltwater effect after 100 years of freshwater forcing increases from ~0.2‰ (5%) in the 0.10 Sv experiment to ~3‰ (35%) in the 1.00 Sv experiment. This increase is more pronounced for stronger hosing because the indirect effect in Greenland saturates for freshwater forcing greater than 0.25 Sv (Figure S1), due to the minimum in AMOC intensity and negative feedbacks associated with surface temperature (e.g., long-wave radiation and lapse rate) (Table 1). As a result, there is a greater contribution from the direct meltwater effect over Greenland as the freshwater forcing in the northern North Atlantic becomes larger, especially for stronger hosing cases when the AMOC collapses. Similarly, the direct meltwater effect also becomes more prominent in eastern Brazil  $\delta^{18}\text{O}_p$  with a larger freshwater forcing, with an increase from 0% in the 0.10 Sv experiment to ~75% (2.1‰) in the 1.00 Sv experiment.

These features of the increased contribution of the direct meltwater effect are most apparent when the direct meltwater effect is plotted against the decrease of the AMOC (Figures 2c and 2f). The direct meltwater effect in Greenland and eastern Brazil increases dramatically after the AMOC severely weakens (e.g., a weakening greater than 75%). These results suggest that the direct meltwater effect could be substantial in  $\delta^{18}\text{O}$  reconstructions from Greenland ice cores (>20%) and eastern Brazil speleothem  $\delta^{18}\text{O}$  records (>40%) for a collapse of AMOC caused by meltwater. Thus far, evidence from the Pa/Th ratios in ocean sediments seems to support the existence of a major disruption and collapses of the AMOC during the last glacial cycle (Böhm et al., 2015; Henry et al., 2016; McManus et al., 2004) likely associated with freshwater forcing (Clement & Peterson, 2008). Our study therefore highlights a potentially important role of the direct meltwater effect in interpreting oxygen-isotope records over the last deglaciation.

In order to assess the sensitivity of the direct meltwater effect to the location of the freshwater forcing, we superimpose in Figure 2 the contributions of the direct meltwater effect in experiments wherein meltwater (0.50 Sv) is discharged into the Gulf of Mexico and the Weddell Sea. When the freshwater forcing is applied to the Gulf of Mexico, the difference in the contribution of the direct meltwater effect over Greenland and eastern Brazil from the northern North Atlantic case is within 5–10% (see also Figure S5 in the supporting information). Adding meltwater into the Weddell Sea does not cause large changes in the total  $\delta^{18}\text{O}_p$  (< 0.5‰ for 0.50 Sv freshwater forcing) over Greenland and eastern Brazil (Figures 2a, 2d, and S5). We argue that the direct meltwater effect is nonnegligible in Greenland ice core  $\delta^{18}\text{O}$  records as long as the meltwater is discharged into any location in the North Atlantic, the Arctic Ocean, or even the North Pacific Ocean, because these are the major moisture source regions for precipitation over Greenland (see also Table S1 in the supporting information) (Charles et al., 1994; Rhines & Huybers, 2014; Sime et al., 2013; Sodemann et al., 2008; Werner, Mikolajewicz, Heimann, Hofmann, 2000). Similarly, the direct meltwater effect could significantly influence the eastern Brazil  $\delta^{18}\text{O}$  records, as long as the meltwater can be easily transported to the moisture source regions such as the tropical North and South Atlantic (Table S1) (Drumond et al., 2008; Lewis et al., 2010). We caution that experiments with freshwater forcing discharged into the Gulf of

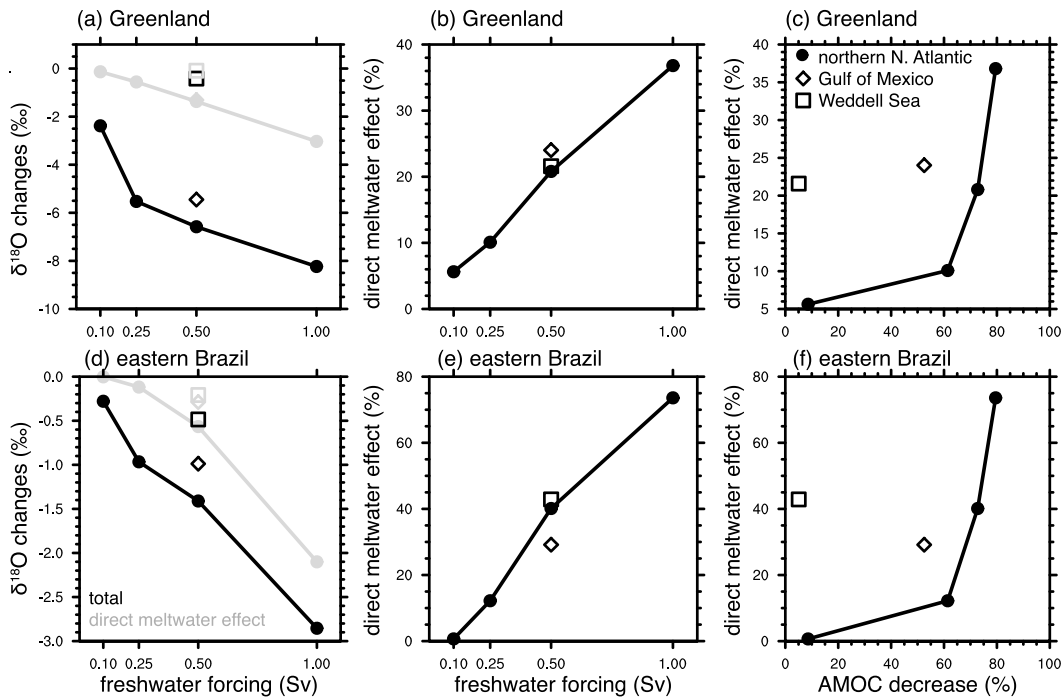


**Figure 2.** (a) Total changes (black) of the annual mean  $\delta^{18}\text{O}$  in precipitation averaged over Greenland and the direct meltwater effect (gray) in water hosing experiments with meltwater discharged into the northern North Atlantic (dots), the Gulf of Mexico (diamonds), and the Weddell Sea (squares). (b) The direct meltwater effect in percentage in different water hosing experiments. (c) The direct meltwater effect versus the AMOC decrease in percentage. (d, e, f) The same as Figures 2a–2c but for eastern Brazil. Calculations are based on model output averaged between model year 91 and 100.

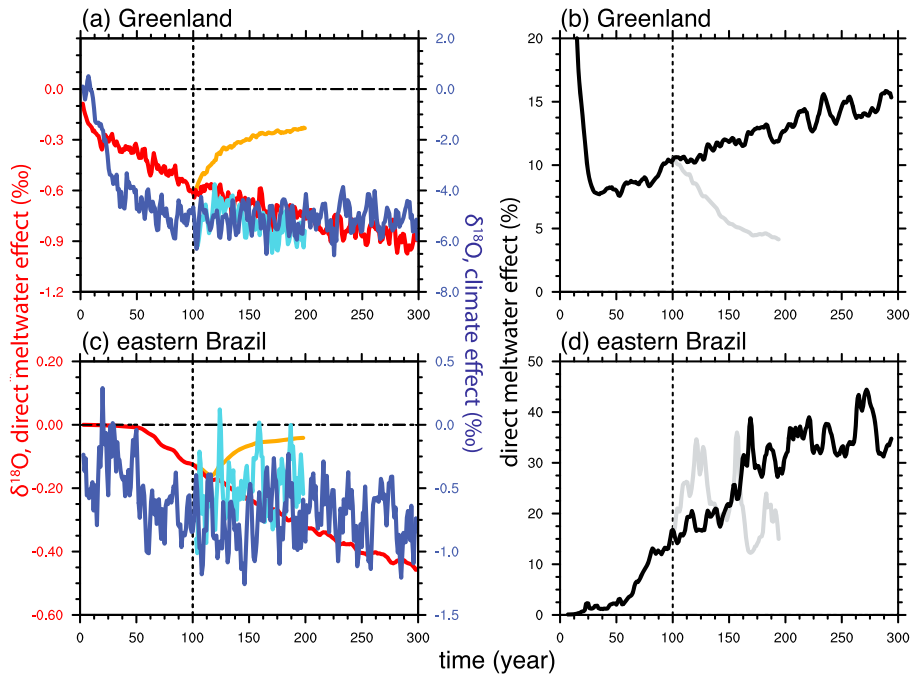


**Figure 3.** (a) Time series of the simulated direct meltwater effect (red, left axis) and the climate effect (blue, right axis) in Greenland in the WH025a experiment. (b) Time series of the direct meltwater effect in percentage. (c, d) The same as Figures 3a and 3b but for eastern Brazil. Time series of the additional experiment with the freshwater forcing removed at year 101 are plotted as orange lines for the direct meltwater effect and cyan for the climate effect in Figures 3a and 3c and gray lines for the direct meltwater effect in percentage in Figures 3b and 3d.

Mexico and Antarctic have not reached quasi-equilibrium in 100 years (Figure S1). If we integrate the experiments further, the contribution of the direct meltwater effect could be larger.

Finally, the importance of the direct meltwater effect increases gradually with the increase of the duration of meltwater discharge in the northern North Atlantic. As shown in Figure 3, the direct meltwater effect averaged over Greenland in the 0.25 Sv experiment increases almost linearly from about  $-0.6\text{‰}$  (10%) at year 100 to about  $-0.9\text{‰}$  (15%) at year 300 (Figure 3a, left axis), due to the slow redistribution of  $^{18}\text{O}$ -depleted meltwater by the hydrological cycle in the model. In contrast, the indirect climate effect in Greenland reaches saturation in the first 70–80 years after the introduction of the meltwater (Figure 3a, right axis). Similarly, the direct meltwater effect over eastern Brazil also increases with the duration of the freshwater forcing from about 15% at year 100 to 35% at year 300. Furthermore, if the freshwater forcing terminates after 100 years in the modeling runs (orange, cyan, and gray lines in Figure 3), the direct meltwater effect over Greenland decreases rapidly to less than  $-0.2\text{‰}$  (5%) in 50 years, while the climate effect remains unchanged. In eastern Brazil, the direct meltwater effect starts to decrease after  $\sim 50$  years. The transient nature of the direct meltwater effect makes it challenging to quantify in oxygen-isotope records, especially when the details (magnitude, location, and duration) of freshwater forcing in the past are currently poorly constrained by reconstructions (Clark et al., 2001).

## 6. Conclusions and Discussion

In summary, we find that a portion of the  $\delta^{18}\text{O}$  signals in terrestrial oxygen-isotope paleoclimate records during meltwater events can be attributed to the direct propagation of the  $^{18}\text{O}$ -depleted meltwater by the hydrological cycle (the direct meltwater effect), without involving changes in local temperature, precipitation amount, or circulations (the climate effects). For a freshwater forcing of 0.25 Sv lasting 300 years in the North Atlantic, the direct meltwater effect contributes more than 15% (about  $1.0\text{‰}$ ) of the total  $\delta^{18}\text{O}$  depletion in Greenland and at least 25% ( $0.4\text{‰}$ ) of the total  $\delta^{18}\text{O}$  depletion in eastern Brazil in our modeling experiments. The contribution of the direct meltwater effect to the total  $\delta^{18}\text{O}$  signals is dependent on the magnitude, location, and duration of the freshwater forcing. In both Greenland and eastern Brazil, the direct meltwater effect at year 100 increases almost linearly with the magnitude of the freshwater forcing over the northern North Atlantic, from approximately 5% and 0% in the 0.10 Sv experiment to about 35% and 75% in the 1.00 Sv experiment, respectively. This linearity is largely because the direct meltwater effect is constrained only by the total amount of freshwater input, while the indirect climate effects are also constrained by climate dynamics, including thresholds related to the AMOC having a lower limit, such that additional freshwater forcing produces no meaningful changes in the oceanic overturning circulation or its impact on the climate system. The direct meltwater effect also increases gradually with the duration of meltwater discharge, but the effect ends in decades over Greenland once the freshwater forcing ceases. Furthermore, the direct meltwater effect still contributes a substantial amount to the total  $\delta^{18}\text{O}$  changes over Greenland and eastern Brazil when the freshwater forcing is applied to the Gulf of Mexico but becomes trivial when the forcing is added to the Weddell Sea.

Aside from Greenland and eastern Brazil, the direct meltwater effect is also found to be significant for other regions, for example, its contribution over the North America and downstream in high-latitude Eurasia continent exceeding 50%. Our modeling results suggest that simple climatic interpretations of the  $\delta^{18}\text{O}$  records in these regions could overestimate the climate signal, especially for the strongest meltwater events with large and long-lasting meltwater discharges. Interestingly, the direct meltwater effect can be opposite in sign to the climate effects, such as over the Caribbean, West Africa, and East and South Asia. This opposing  $\delta^{18}\text{O}$  effect may potentially mask part of the climatic effects and therefore lead to an underestimation of the climate signal during meltwater events in records from these regions.

The direct meltwater effect occurs in certain locations because the  $^{18}\text{O}$ -depleted meltwater discharged into the ocean can alter the  $\delta^{18}\text{O}$  over the moisture source regions for that location. Water tagging experiments demonstrate that moisture originating from the North Atlantic contributes up to 58% and 15% of the precipitation over Greenland and eastern Brazil, respectively (Table S1). Thus, we argue that the direct meltwater effect could also be significant for other meltwater scenarios and in other terrestrial oxygen-isotope records, as long as the meltwater is discharged into or can be easily transported to the major moisture source of the  $\delta^{18}\text{O}_p$  record sites.

We note that these water hosing experiments are idealized, in an effort to concisely capture the relative contributions of the direct meltwater and indirect climatic effects. Related to this, we note further that our ocean model resolution is still too coarse to sufficiently resolve boundary processes that could be important for transporting freshwater from near-shore regions to the open ocean (Condrón & Winsor, 2011; Keigwin et al., 2005). Simulations with much higher resolution should be performed to fully resolve the behavior of freshwater from near-shore regions to the open ocean and to reevaluate the direct meltwater effect for meltwater routing events. The direct meltwater effect could also depend on the background climate state, that is, glacial versus interglacial conditions. Nevertheless, previous studies (Brady et al., 2013; He, 2011; Hu et al., 2008; Otto-Bliesner & Brady, 2010) suggest that a glacial boundary condition would induce similar climatic responses to freshwater forcing and is unlikely to substantially affect our results. Simulations using multiple water isotope-enabled climate models are also needed to further quantify the uncertainty of the direct meltwater effect for different regions and characteristics of freshwater forcing. Moreover, necessary caution should be taken when interpreting the model results, as the exact contribution of the direct meltwater effect in speleothem records could be compromised by multiple processes impacting stalagmite carbonate  $\delta^{18}\text{O}$ , including drip water  $\delta^{18}\text{O}$ , cave temperature, and complicated cave hydrological, and geochemical processes (Fairchild et al., 2006).

Nonetheless, our modeling experiments clearly identify a largely underappreciated, nonclimatic portion of the  $\delta^{18}\text{O}$  signal in terrestrial-based reconstructions during meltwater events and suggest that previous climatic interpretations of these  $\delta^{18}\text{O}$  records may have been overestimated or underestimated, especially for strong meltwater events. The dependence of the direct meltwater effect on the details of freshwater forcing calls for future studies to obtain a robust detailed history of meltwater flux, in order for an accurate climatic interpretation of the  $\delta^{18}\text{O}$  in terrestrial paleoclimate records.

#### Acknowledgments

This work is supported by NSF P2C2 awards AGS-1401778/1401803/1401802 and NSF41630527. We thank David Bailey, Erik Kluzek, and Mariana Vertenstein for their contributions to developing and testing the iCESM. The National Center for Atmospheric Research (NCAR) is sponsored by the U.S. National Science Foundation (NSF). J. Zhang is supported by U.S. DOE the RGCM program and the CNLS sponsored by LDRD. A. J. is supported by the NSF-P2C2 award 1566432. We would like to acknowledge high-performance computing support from Yellowstone (ark:/85065/d7wd3xhc) provided by NCAR's Computational and Information Systems Laboratory, sponsored by the National Science Foundation. The iCESM model codes are available through the National Center for Atmospheric Research software development repository. Data for simulations in this paper can be requested by sending e-mail to J. Z. (jzhu47@wisc.edu).

#### References

- Aggarwal, P. K., Romatschke, U., Araguas-Araguas, L., Belachew, D., Longstaffe, F. J., Berg, P., ... Funk, A. (2016). Proportions of convective and stratiform precipitation revealed in water isotope ratios. *Nature Geoscience*, *9*, 624–629.
- Andersen, K. K., Azuma, N., Barnola, J. M., Bigler, M., Biscaye, P., Caillon, N., ... White, J. (2004). High-resolution record of Northern Hemisphere climate extending into the last interglacial period. *Nature*, *431*(7005), 147–151. <https://doi.org/10.1038/nature02805>
- Bagniewski, W., Meissner, K. J., & Menviel, L. (2017). Exploring the oxygen isotope fingerprint of Dansgaard-Oeschger variability and Heinrich events. *Quaternary Science Reviews*, *159*, 1–14. <https://doi.org/10.1016/j.quascirev.2017.01.007>
- Bagniewski, W., Meissner, K. J., Menviel, L., & Brennan, C. E. (2015). Quantification of factors impacting seawater and calcite  $\delta^{18}\text{O}$  during Heinrich Stadials 1 and 4. *Paleoceanography*, *30*, 895–911. <https://doi.org/10.1002/2014PA002751>
- Böhm, E., Lippold, J., Gutjahr, M., Frank, M., Blaser, P., Antz, B., ... Deininger, M. (2015). Strong and deep Atlantic meridional overturning circulation during the last glacial cycle. *Nature*, *517*(7534), 73–76. <https://doi.org/10.1038/nature14059>
- Brady, E. C., & Otto-Bliesner, B. L. (2011). The role of meltwater-induced subsurface ocean warming in regulating the Atlantic meridional overturning in glacial climate simulations. *Climate Dynamics*, *37*(7–8), 1517–1532. <https://doi.org/10.1007/s00382-010-0925-9>
- Brady, E. C., Otto-bliesner, B. L., Kay, J. E., & Rosenbloom, N. (2013). Sensitivity to glacial forcing in the CCSM4. *Journal of Climate*, *26*(6), 1901–1925. <https://doi.org/10.1175/JCLI-D-11-00416.1>
- Broecker, W. S. (1992). The great ocean conveyor. *AIP Conference Proceedings*, *247*(2), 129–161. <https://doi.org/10.1063/1.41925>
- Carolin, S. A., Cobb, K. M., Adkins, J. F., Clark, B., Conroy, J. L., Lejau, S., ... Tuen, A. a. (2013). Varied response of western Pacific hydrology to climate forcings over the last glacial period. *Science*, *340*(6140), 1564–1566. <https://doi.org/10.1126/science.1233797>
- Charles, C. D., Rind, D., Jouzel, J., Koster, R. D., & Fairbanks, R. G. (1994). Glacial-interglacial changes in moisture sources for Greenland: Influences on the ice core record of climate. *Science*, *263*(5146), 508–511.
- Cheng, H., Edwards, R. L., Broecker, W. S., Denton, G. H., Kong, X., Wang, Y., ... Wang, X. (2009). Ice age terminations. *Science*, *326*(5950), 248–252.
- Clark, P. U., Marshall, S. J., Clarke, G. K. C., Hostetler, S. W., Licciardi, J. M., & Teller, J. T. (2001). Freshwater forcing of abrupt climate change during the last glaciation. *Science*, *293*(5528), 283–287.
- Clark, P. U., McCabe, A. M., Mix, A. C., & Weaver, A. J. (2004). Rapid rise of sea level 19,000 years ago and its global implications. *Science*, *304*(5674), 1141–1144. <https://doi.org/10.1126/science.1094449>
- Clement, A. C., & Peterson, L. C. (2008). Mechanisms of abrupt climate change of the last glacial period. *Reviews of Geophysics*, *46*, RG4002. <https://doi.org/10.1029/2006RG000204>
- Condrón, A., & Winsor, P. (2011). A subtropical fate awaited freshwater discharged from glacial Lake Agassiz. *Geophysical Research Letters*, *38*, L03705. <https://doi.org/10.1029/2010GL046011>
- Cruz, F. W., Burns, S. J., Karmann, I., Sharp, W. D., Vuille, M., & Ferrari, J. A. (2006). A stalagmite record of changes in atmospheric circulation and soil processes in the Brazilian subtropics during the Late Pleistocene. *Quaternary Science Reviews*, *25*(21–22), 2749–2761. <https://doi.org/10.1016/j.quascirev.2006.02.019>
- Cruz, F. W., Vuille, M., Burns, S. J., Wang, X., Cheng, H., Werner, M., ... Nguyen, H. (2009). Orbitally driven east-west antiphasing of South American precipitation. *Nature Geoscience*, *2*(3), 210–214. <https://doi.org/10.1038/ngeo444>
- Dansgaard, W. (1964). Stable isotopes in precipitation. *Tellus*, *16*(4), 436–468. <https://doi.org/10.3402/tellusa.v16i4.8993>
- Drummond, A., Nieto, R., Gimeno, L., & Ambrizzi, T. (2008). A Lagrangian identification of major sources of moisture over Central Brazil and La Plata Basin. *Journal of Geophysical Research*, *113*, D14128. <https://doi.org/10.1029/2007JD009547>



- Fairchild, I. J., Smith, C. L., Baker, A., Fuller, L., Spötl, C., Matthey, D., & McDermott, F. (2006). Modification and preservation of environmental signals in speleothems. *Earth-Science Reviews*, 75(1-4), 105–153. <https://doi.org/10.1016/j.earscirev.2005.08.003>
- Groote, P. M., Stuiver, M., White, J. W. C., Johnsen, S., & Jouzel, J. (1993). Comparison of oxygen isotope records from the GISP2 and GRIP Greenland ice cores. *Nature*, 366(6455), 552–554. <https://doi.org/10.1038/366552a0>
- He, F. (2011). *Simulating transient climate evolution of the last deglaciation with CCSM3* (185 pp.). Madison, WI: The University of Wisconsin - Madison.
- Heinrich, H. (1988). Origin and consequences of cyclic ice rafting in the Northeast Atlantic Ocean during the past 130,000 years. *Quaternary Research*, 29(02), 142–152. [https://doi.org/10.1016/0033-5894\(88\)90057-9](https://doi.org/10.1016/0033-5894(88)90057-9)
- Hemming, S. R. (2004). Heinrich events: Massive late Pleistocene detritus layers of the North Atlantic and their global climate imprint. *Reviews of Geophysics*, 42, RG1005. <https://doi.org/10.1029/2003RG000128>
- Hendricks, M. B., DePaolo, D. J., & Cohen, R. C. (2000). Space and time variation of  $\delta^{18}\text{O}$  and  $\delta\text{D}$  in precipitation: Can paleotemperature be estimated from ice cores? *Global Biogeochemical Cycles*, 14, 851–861. <https://doi.org/10.1029/1999GB001198>
- Henry, L. G., Henry, L. G., McManus, J. F., Curry, W. B., Roberts, N. L., Piotrowski, A. M., & Keigwin, L. D. (2016). North Atlantic ocean circulation and abrupt climate change during the last glaciation. *Science*, 353(6298), 470–474. <https://doi.org/10.1126/science.aaf5529>
- Hillaire-Marcel, C., & Causse, C. (1989). The late Pleistocene Laurentide glacier: Th U dating of its major fluctuations and  $\delta^{18}\text{O}$  range of the ice. *Quaternary Research*, 32(02), 125–138. [https://doi.org/10.1016/0033-5894\(89\)90070-7](https://doi.org/10.1016/0033-5894(89)90070-7)
- Hu, A., Otto-Bliesner, B. L., Meehl, G. A., Han, W., Morrill, C., Brady, E. C., & Briegleb, B. (2008). Response of thermohaline circulation to freshwater forcing under present-day and LGM conditions. *Journal of Climate*, 21(10), 2239–2258. <https://doi.org/10.1175/2007JCLI1985.1>
- Hurrell, J. W., Holland, M. M., Gent, P. R., Ghan, S., Kay, J. E., Kushner, P. J., ... Marshall, S. (2013). The community Earth system model: A framework for collaborative research. *Bulletin of the American Meteorological Society*, 94(9), 1339–1360. <https://doi.org/10.1175/BAMS-D-12-00121.1>
- Johnsen, S. J., Dahl-Jensen, D., Gundestrup, N., Steffensen, J. P., Clausen, H. B., Miller, H., ... White, J. (2001). Oxygen isotope and palaeotemperature records from six Greenland ice-core stations: Camp Century, Dye-3, GRIP, GISP2, Renland and NorthGRIP. *Journal of Quaternary Science*, 16(4), 299–307. <https://doi.org/10.1002/jqs.622>
- Jouzel, J., Alley, R. B., Cuffey, K. M., Dansgaard, W., Groote, P., Hoffmann, G., ... White, J. (1997). Validity of the temperature reconstruction from water isotopes in ice cores. *Journal of Geophysical Research*, 102, 26,471–26,487. <https://doi.org/10.1029/97JC01283>
- Keigwin, L. D., Sachs, J. P., Rosenthal, Y., & Boyle, E. A. (2005). The 8200 year B.P. event in the slope water system, western subpolar North Atlantic. *Paleoceanography*, 20, PA2003. <https://doi.org/10.1029/2004PA001074>
- Kim, S.-T., & O'Neil, J. R. (1997). Equilibrium and nonequilibrium oxygen isotope effects in synthetic carbonates. *Geochimica et Cosmochimica Acta*, 61(16), 3461–3475. [https://doi.org/10.1016/S0016-7037\(97\)00169-5](https://doi.org/10.1016/S0016-7037(97)00169-5)
- Lee, J.-E., Fung, I., DePaolo, D. J., & Henning, C. C. (2007). Analysis of the global distribution of water isotopes using the NCAR atmospheric general circulation model. *Journal of Geophysical Research*, 112, D16306. <https://doi.org/10.1029/2006JD007657>
- LeGrande, A. N., & Schmidt, G. A. (2006). Global gridded data set of the oxygen isotopic composition in seawater. *Geophysical Research Letters*, 33, L12604. <https://doi.org/10.1029/2006GL026011>
- LeGrande, A. N., & Schmidt, G. A. (2008). Ensemble, water isotope-enabled, coupled general circulation modeling insights into the 8.2 ka event. *Paleoceanography*, 23, PA3207. <https://doi.org/10.1029/2008PA001610>
- LeGrande, A. N., Schmidt, G. A., Shindell, D. T., Field, C. V., Miller, R. L., Koch, D. M., ... Hoffmann, G. (2006). Consistent simulations of multiple proxy responses to an abrupt climate change event. *Proceedings of the National Academy of Sciences of the United States of America*, 103(4), 837–842. <https://doi.org/10.1073/pnas.0510095103>
- Lewis, S. C., Legrande, A. N., Kelley, M., & Schmidt, G. A. (2010). Water vapour source impacts on oxygen isotope variability in tropical precipitation during Heinrich events. *Climate of the Past*, 6(3), 325–343. <https://doi.org/10.5194/cp-6-325-2010>
- Liu, Z., Carlson, A. E., He, F., Brady, E. C., Otto-Bliesner, B. L., Briegleb, B. P., ... Zhu, J. (2012). Younger Dryas cooling and the Greenland climate response to  $\text{CO}_2$ . *Proceedings of the National Academy of Sciences*, 109(28), 11,101–11,104. <https://doi.org/10.1073/pnas.1202183109>
- Liu, Z., Wen, X., Brady, E. C., Otto-Bliesner, B., Yu, G., Lu, H., ... Yang, H. (2014). Chinese cave records and the East Asia Summer Monsoon. *Quaternary Science Reviews*, 83, 115–128. <https://doi.org/10.1016/j.quascirev.2013.10.021>
- McManus, J. F., Francois, R., Gherardi, J. M., Keigwin, L. D., & Brown-Leger, S. (2004). Collapse and rapid resumption of Atlantic meridional circulation linked to deglacial climate changes. *Nature*, 428(6985), 834–837. <https://doi.org/10.1038/nature02494>
- NEEM community members (2013). Eemian interglacial reconstructed from a Greenland folded ice core. *Nature*, 493(7433), 489–494. <https://doi.org/10.1038/nature11789>
- Moore, M., Kuang, Z., & Blossy, P. N. (2014). A moisture budget perspective of the amount effect. *Geophysical Research Letters*, 41, 1329–1335. <https://doi.org/10.1002/2013GL058302>
- Noone, D. (2008). The influence of midlatitude and tropical overturning circulation on the isotopic composition of atmospheric water vapor and Antarctic precipitation. *Journal of Geophysical Research*, 113, D04102. <https://doi.org/10.1029/2007JD008892>
- Nusbaumer, J., Wong, T., Bardeen, C., & Noone, D. (2017). Evaluating hydrological processes in the Community Atmosphere Model Version 5 (CAM5) using stable isotope ratios of water. *Journal of Advances in Modeling Earth Systems*, 9(2), 949–977. <https://doi.org/10.1002/2016MS000839>
- Otto-Bliesner, B. L., & Brady, E. C. (2010). The sensitivity of the climate response to the magnitude and location of freshwater forcing: Last glacial maximum experiments. *Quaternary Science Reviews*, 29(1-2), 56–73. <https://doi.org/10.1016/j.quascirev.2009.07.004>
- Partin, J. W., Cobb, K. M., Adkins, J. F., Clark, B., & Fernandez, D. P. (2007). Millennial-scale trends in west Pacific warm pool hydrology since the Last Glacial Maximum. *Nature*, 449(7161), 452–455. <https://doi.org/10.1038/nature06164>
- Rhines, A., & Huybers, P. J. (2014). Sea ice and dynamical controls on preindustrial and Last Glacial Maximum accumulation in Central Greenland. *Journal of Climate*, 27(23), 8902–8917. <https://doi.org/10.1175/JCLI-D-14-00075.1>
- Risi, C., Bony, S., & Vimeux, F. (2008). Influence of convective processes on the isotopic composition ( $\delta^{18}\text{O}$  and  $\delta\text{D}$ ) of precipitation and water vapor in the tropics: 2. Physical interpretation of the amount effect. *Journal of Geophysical Research*, 113, D19306. <https://doi.org/10.1029/2008JD009943>
- Roche, D. M., Paillard, D., Caley, T., & Waelbroeck, C. (2014). LGM hosing approach to Heinrich Event 1: Results and perspectives from data-model integration using water isotopes. *Quaternary Science Reviews*, 106, 247–261. <https://doi.org/10.1016/j.quascirev.2014.07.020>
- Rozanski, K., Araguás-Araguás, L., & Gonfiantini, R. (1993). *Isotopic patterns in modern global precipitation* (pp. 1–36). Washington, DC: American Geophysical Union.
- Sima, A., Paul, A., Schulz, M., & Oerlemans, J. (2006). Modeling the oxygen-isotopic composition of the North American Ice Sheet and its effect on the isotopic composition of the ocean during the last glacial cycle. *Geophysical Research Letters*, 33, L15706. <https://doi.org/10.1029/2006GL026923>

- Sime, L. C., Risi, C., Tindall, J. C., Sjolte, J., Wolff, E. W., Masson-Delmotte, V., & Capron, E. (2013). Warm climate isotopic simulations: What do we learn about interglacial signals in Greenland ice cores? *Quaternary Science Reviews*, *67*, 59–80. <https://doi.org/10.1016/j.quascirev.2013.01.009>
- Sodemann, H., Schwierz, C., & Wernli, H. (2008). Interannual variability of Greenland winter precipitation sources: Lagrangian moisture diagnostic and North Atlantic Oscillation influence. *Journal of Geophysical Research*, *113*, D03107. <https://doi.org/10.1029/2007JD008503>
- Steen-Larsen, H. C., Masson-Delmotte, V., Hirabayashi, M., Winkler, R., Satow, K., Prié, F., ... Sveinbjörnsdóttir, A. E. (2014). What controls the isotopic composition of Greenland surface snow? *Climate of the Past*, *10*(1), 377–392. <https://doi.org/10.5194/cp-10-377-2014>
- Stouffer, R. J., Yin, J., Gregory, J. M., Dixon, K. W., Spelman, M. J., Hurlin, W., ... Weber, S. L. (2006). Investigating the cause of the response of the thermohaline circulation to past and future climate changes. *Journal of Climate*, *19*(8), 1365–1387. <https://doi.org/10.1175/JCLI3689.1>
- Strikis, N. M., Chiessi, C. M., Cruz, F. W., Vuille, M., Cheng, H., de Souza Barreto, E. A., ... Sales, H. R. (2015). Timing and structure of Mega-SACZ events during Heinrich Stadial 1. *Geophysical Research Letters*, *42*, 5477–5484. <https://doi.org/10.1002/2015GL064048>
- Tierney, J. E., Russell, J. M., Huang, Y., Damsté, J. S. S., Hopmans, E. C., & Cohen, A. S. (2008). Northern Hemisphere controls on tropical southeast African climate during the past 60,000 years. *Science*, *322*(5899), 252–255. <https://doi.org/10.1126/science.1160485>
- Town, M. S., Warren, S. G., Walden, V. P., & Waddington, E. D. (2008). Effect of atmospheric water vapor on modification of stable isotopes in near-surface snow on ice sheets. *Journal of Geophysical Research*, *113*, D24303. <https://doi.org/10.1029/2008JD009852>
- Wang, X., Auler, A. S., Edwards, R. L., Cheng, H., Ito, E., Wang, Y., ... Solheid, M. (2007). Millennial-scale precipitation changes in southern Brazil over the past 90,000 years. *Geophysical Research Letters*, *34*, L23701. <https://doi.org/10.1029/2007GL031149>
- Wang, Y., Cheng, H., Edwards, R. L., Kong, X., Shao, X., Chen, S., ... An, Z. (2008). Millennial- and orbital-scale changes in the East Asian monsoon over the past 224,000 years. *Nature*, *451*(7182), 1090–1093. <https://doi.org/10.1038/nature06692>
- Wang, Y. J., Cheng, H., Edwards, R. L., An, Z. S., Wu, J. Y., Shen, C. C., & Dorale, J. A. (2001). A high-resolution absolute-dated Late Pleistocene monsoon record from Hulu Cave, China. *Science*, *294*(5550), 2345–2348. <https://doi.org/10.1126/science.1064618>
- Werner, M., Mikolajewicz, U., Heimann, M., & Hoffmann, G. (2000). Borehole versus isotope temperatures on Greenland: Seasonality does matter. *Geophysical Research Letters*, *27*, 723–726. <https://doi.org/10.1029/1999GL006075>
- Werner, M., Mikolajewicz, U., Hoffmann, G., & Heimann, M. (2000). Possible changes of  $\delta^{18}\text{O}$  in precipitation caused by a meltwater event in the North Atlantic. *Journal of Geophysical Research*, *105*, 10,161–10,167. <https://doi.org/10.1029/1999JD901196>
- Wong, T., Nusbaumer, J., & Noone, D. (2017). Evaluation of modeled land-atmosphere exchanges with a comprehensive water isotope fractionation scheme in version 4 of the Community Land Model. *Journal of Advances in Modeling Earth Systems*, *9*(2), 978–1001. <https://doi.org/10.1002/2016MS000842>
- Yuan, D., Cheng, H., Edwards, R. L., Dykoski, C. A., Kelly, M. J., Zhang, M., ... Cai, Y. (2004). Timing, duration, and transitions of the Last Interglacial Asian Monsoon. *Science*, *304*(5670), 575–578. <https://doi.org/10.1126/science.1091220>
- Zhang, J., Liu, Z., Brady, E. C., Oppo, D. W., Clark, P. U., Jahn, A., ... Lindsay, K. (2017). Asynchronous warming and  $\delta^{18}\text{O}$  evolution of deep Atlantic water masses during the last deglaciation. *Proceedings of the National Academy of Sciences*, *114*(42), 11075–11080. <https://doi.org/10.1073/pnas.1704512114>
- Zhou, H., Zhao, J., Feng, Y., Gagan, M. K., Zhou, G., & Yan, J. (2008). Distinct climate change synchronous with Heinrich event one, recorded by stable oxygen and carbon isotopic compositions in stalagmites from China. *Quaternary Research*, *69*(02), 306–315. <https://doi.org/10.1016/j.yqres.2007.11.001>
- Zhu, J., Liu, Z., Brady, E., Otto-Bliesner, B., Zhang, J., Noone, D., ... Tabor, C. (2017). Reduced ENSO variability at the LGM revealed by an isotope-enabled Earth system model. *Geophysical Research Letters*, *44*, 6984–6992. <https://doi.org/10.1002/2017GL073406>